Universidad de Concepción
Facultad de Ingeniería

DOUBLE-LOUVER GATE FOR FLOW CONTROL IN FLUMES

COMPUERTA DE DOBLE PERSIANA PARA EL CONTROL DEL FLUJO EN CANALES ARTIFICIALES

POR
NICOLÁS GATICA RUIZ

Tesis presentada a la Facultad de Ingeniería de la Universidad de Concepción para optar al grado de Magíster en Ciencias de la Ingeniería con Mención Ingeniería Civil

PROFESOR GUÍA
OSCAR LINK LAZO

CONCEPCIÓN, CHILE 2021

ABSTRACT

The downstream border condition of an open channel, subcritical flow in a laboratory flume is typically materialized through a gate, which imposes a gradually varied conditions upstream. A number of different gates are used for flow control, but the flow alteration they produce in most cases is unknown. In this paper, we analyze the effects of a double louver gate on the upstream flow in a laboratory flume. The flow properties are measured through a particle image velocimetry. Vertical velocity profiles, recirculation zones, and turbulent kinetic energy distributions are analyzed. Results show that the double louver gate is less flow-altering than the common vertical sluice gate, being best suited for the outflow control in flumes, as it conserves parallel streamlines, with a minimum deformation of the vertical velocity profiles, avoiding the formation of recirculation zones and concentrations of turbulent kinetic energy. The double-louver gate is recommended for its implementation in hydraulic laboratories.

to my parents Juana and Luis…

ACKNOWLEDGEMENTS

I would like to express my gratitude to my professor Oscar Link for his support and guidance in this project. To René Iribarren for his help and collaboration in experimental setup. I would like to extend this gratitude to María José Valdés and Gustavo Vigueras for accompany me virtually along nocturne sessions. And finally, to my family for always motivated me.

CONTENTS

LIST OF TABLES

LIST OF FIGURES

CHAPTER 1. INTRODUCTION

1.1. Motivation

Experimental research in open channel flow is massively conducted in laboratory flumes. For a given discharge, bulk properties of subcritical flow, i.e. flow depth and flow velocity, are adjusted through an endgate, imposing a gradually varied flow upstream. A number of different gates are available for this purpose, such as radial gates, vertical, and inclined sluice gates. One of the most common kind of gate for flow control in laboratory flumes is the vertical sluice gate, which consists in a moveable plate that is raised to adjust its lower opening in order to measure or regulate flow discharge and water depth (Boiten, 2002).

In practice, effects of endgates on the upstream flow field are neglected, provided that experimental observations are performed at a reasonable distance from the gate. However, the flow alteration by different kind of gates is unknown, introducing uncertainties in experimental results (Muste *et al.*,2017), and undesired approximations in the mathematical representation of border conditions defining the hydrodynamic problem (Dazzi *et al.*, 2020).

In order to minimize uncertainty of upstream effect and maximize reliability in experimentation and definition of border conditions, a new kind of gate with homogeneous blockage of the flow is needed.

1.2. Hypothesis

We hypothesize that a gate producing a homogenous blockage of the flow, is expected to induce less alteration of the flow field than gates partially blocking the flow section, like e.g. the sluice gate.

1.3. Objectives

1.3.1. General Objective

Analyze upstream effect of double louver gate and vertical sluice gate.

1.3.2. Specific Objectives

- Assemble an experimental installation to record the particle motion at different distances upstream from the gates.
- Process experimental data obtained and extract upstream flow characteristics.

- Identify main characteristics disturb upstream flow conditions.
- Quantify the effect of each gate in those conditions.

1.4. Methodology

In this work a two-dimensional Particle Image Velocimetry (PIV) was the technique chosen to measure flow characteristics at different distances upstream from a vertical sluice gate. To proof the hypothesis, the effects of a double-louver gate on the upstream flow in a laboratory flume are analyzed.

1.5. Structure of the thesis

In the next section a review of state of art is exhibit. Section 3 presents the experimental installation, measuring techniques, and experimentation details. Then Chapter 4 presents the flow properties, including identification of recirculation zones, vertical velocity profiles, and distribution of turbulent kinetic energy. Final section concludes with final remarks on the obtained results.

CHAPTER 2. THEORICAL BACKGROUND

2.1. Introduction

In this chapter, a theorical background about open channel flows and upstream effect of a sluice gate are presented. Also, PIV measurement technique are described.

2.2. Velocity profile in open channel flows

As is already known the velocity of flow at any channel section is not constant with depth. It increases from zero at the bottom of the channel (stagnation point) to a maximum value close to the water surface. This is due to the presence of free surface and frictional resistance (viscosity) along the channel boundary. Figure 2.1 illustrate an open channel flow scheme.

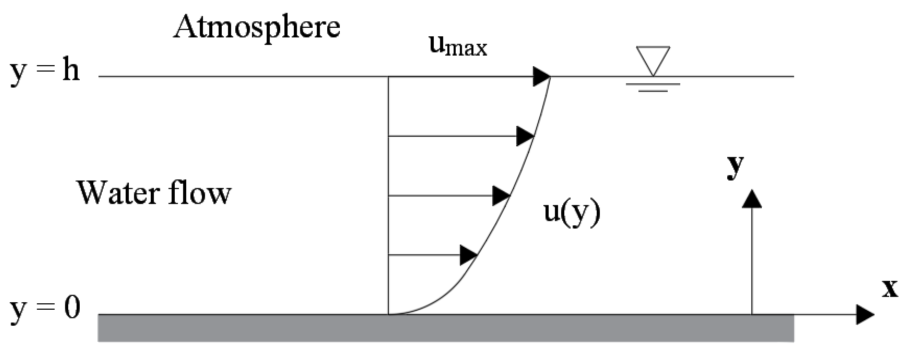

Figure 2.1 Open channel flow schematization.

2.2.1. Viscosity

Viscosity is a quantitative measure of a fluid's resistance to flow. More specifically, it determines the fluid strain rate that is generated by a given applied shear stress. The shear stress is proportional to the slope of the velocity profile and is greatest at the wall. Further, at the wall, the velocity u is zero relative to the wall: This is called the no-slip condition. The region where the wall exerts an influence on the velocity profile is called boundary layer. The viscosity of Newtonian fluids is a true thermodynamic property and varies with temperature and pressure. Generally speaking, the viscosity of a fluid increases only weakly with pressure. Temperature, however, has a strong effect, with viscosity increasing with it for gases and decreasing for liquids (White, 2003). In a large number of real flow situations, neither viscous nor turbulent shear can be sad to originate a force resisting motion; they merely transmit such a force from its origin, which is often on a solid surface. It is well established by observation that fluid actually in contact with a solid surface has no motion along the surface; the transverse velocity gradient so created enables the solid surface to exert on the moving fluid drag force which is transmitted outwards through successive faster-moving fluid layers. Flow resistance therefore depends as much on the presence of solid surfaces as on the strength of the viscosity or turbulence. Accordingly, if one solid surface is isolated in a large expanse of moving fluid the effects of resistance are confined toa fluid layer of limited thickness adjacent to the surface called boundary layer (Henderson, 1996). Figure 2.2 presents boundary layer behavior.

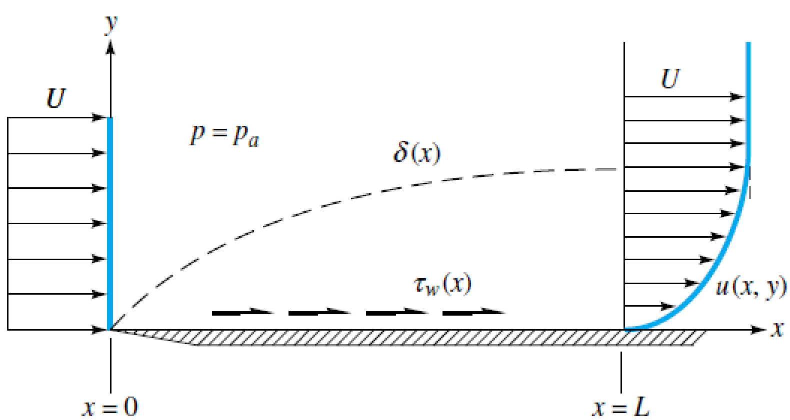

Figure 2.2 Growth of a boundary layer on a flat plate (White, 2003).

Establishing that δ is the boundary layer thickness as the locus of points where the velocity u parallel to the plate reaches 99 percent of the external velocity U. The accepted formulas for flat-plate flow are

$$\frac{\delta}{x} \approx \begin{cases} \dfrac{5.0}{Re_x^{1/2}} & laminar \\ \dfrac{0.16}{Re_x^{1/7}} & turbulent \end{cases} \tag{2.1}$$

2.3. Sluice gate

Sluice gates are underflow structures used for stopping or regulating flow. They are classified into different categories based on different criteria. Based on the downstream water level, they are classified as sluice gate discharging free and submerged flow (Rady, 2016). The outflow is said to be free when the issuing jet of supercritical flow is open to atmosphere and is not overlaid, or submerged, by tailwater of excessive depth. While the submerged outflow occurs when the jet of water issuing from beneath the gate is overlaid by a mass of water which, although strongly turbulent, has not met motion in any direction (Henderson, 1966). Figure 2.2 shows both flow conditions.

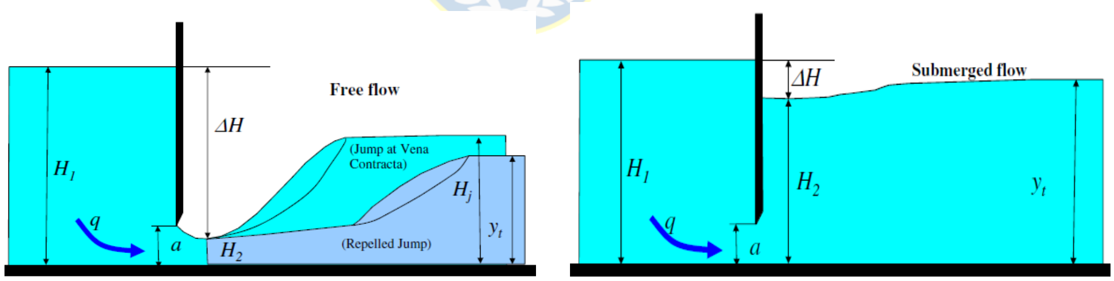

Figure 2.3 Free flow condition (left). Submerged flow condition (right) (Wu and Rajaratnam, 2015).

While, on the basis of alignment with channel axis classified them as normal sluice gate, if the gate is normal to the axis of the channel, side sluice gate, if the gate is parallel to the axis of the channel, and skew sluice gate when the gate is inclined to the axis of the channel. Further, a gate inclined with vertical is classified as inclined or planar gate (Rady, 2016). Particularly, the vertical or normal sluice gate have been widely studied due is the most utilized for laboratory measurements and experimentation.

2.4. Vertical Sluice Gate (VSG)

This gate consists in a moveable plate that is raised to adjust its lower opening in order to measure or regulate flow discharge and water depth. This control device received a lot of attention of many researchers and academics. Rajaratnam and Subramanya (1967a) developed a general equation for predicting the flow under a vertical sluice gate in a rectangular channel for free as well as submerged conditions using momentum equation. Also, they investigated experimentally the velocity and pressure field immediately below a deeply submerged sluice gate located in a rectangular open channel (Rajaratnam and Subramanya, 1967b). Rajaratnam (1977) carried out an experimental study for free flow condition and found that the water surface profiles, immediately below sluice gates in rectangular channels, are similar. He also found that coefficient of contraction was larger than the theoretically predicted value and it is not possible to attribute that difference to boundary layer effects alone. Rajaratnam and Humphries (1982) performed first experimental study considered the free flow characteristics upstream of a vertical gate. They found interesting characteristics of velocity profile and some geometric features of surface eddy. Masliyah *et al*., (1985) employed a boundary-fitted coordinates method in the evaluation of discharge coefficients as well as the free-surface profiles for vertical sluice gates for an ideal fluid. They predicted some details of flow like velocity profile upstream from the gate. Finnie and Jepson (1991) applied a finite element computer code to turbulent flow under a sluice gate. They carried out experiments and compare vertical and horizontal velocities. Montes (1997) developed method of solution for flow under planar sluice gates and suggested that the discrepancy between experimental and theoretical values of contraction coefficient is due to the energy loss associated with the vortex formation at the upstream region of the gate. Roth and Hager (1999) carried out a detailed project of underflow of sluice gate involving: scale effects, discharge coefficient, surface ridge, features of shock waves, velocity field, bottom and gate pressure distribution, corner vortices and vortex intensities. Also proposed a novel device to reduce shock waves. Shammaa *et al*., (2005) extended a point/line sink solution of potential flow to study the velocity field upstream of a finite-size orifice and sluice gate. Akoz *et al*. (2009) conducted laboratory experiments to measure the velocities of 2D turbulent open channel flow upstream of a vertical sluice gate and analyzed it by computational fluid dynamics simulation. Belaud *et al*. (2009) studied the contraction coefficient under sluice gates on flat beds is studied for both free flow and submerged conditions based on the principle of momentum conservation. Cassan and Belaud (2012) investigated experimentally and numerically the flow characteristics upstream and downstream of sluice gates using Reynolds averaged Navier-Stokes two-dimensional simulations with a volume of fluid method. Some characteristics are shown in Figure 2.4.

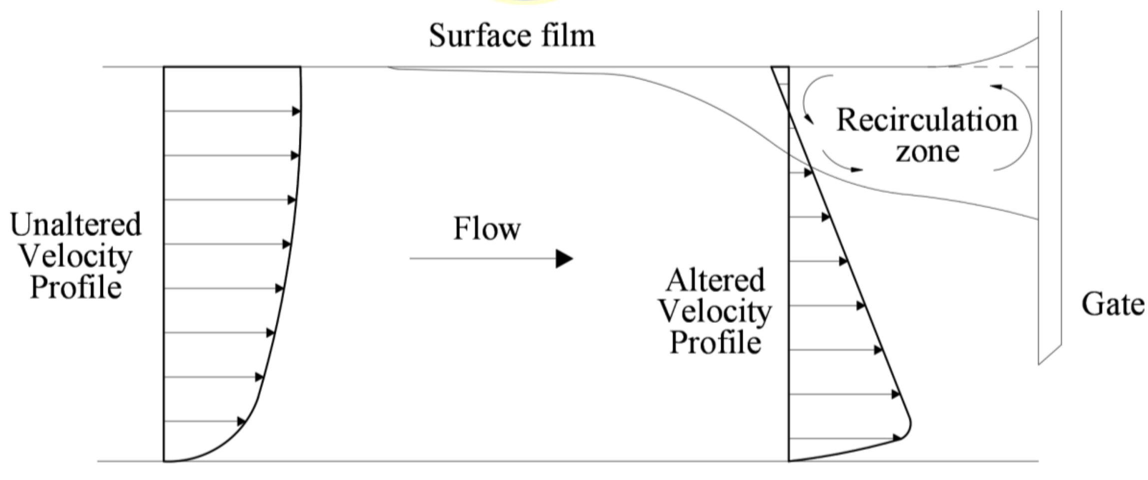

Figure 2.4 Flow characteristics upstream VSG (modified from Rajaratnam and Humphries 1982).

2.4.1. Recirculation zone

Vertical sluice gate opening induces streamlines to go towards bottom of the channel and produces a recirculation zone at upstream region of the gate. Recirculation zone generates a horseshoe vortex or surface eddy and a surface film that extends to a plunging point upstream from the gate. The plunging point of stagnation flow is the so-called Reynold's ridge (Roth and Hager, 1999). It was found that near the thin upstream end of the surface eddy, the flow inside the surface eddy was laminar whereas near the downstream end of the surface eddy, the flow was very turbulent (Rajaratnam and Humphries, 1982).

2.4.2. Surface eddy

The source of the energy loss in all likelihood is the horseshoe-vortex adjacent to the gate. This vortex is formed by the separation of the sidewall boundary layer ahead of the gate due to the local adverse pressure gradient (Montes,1997). For a relative gate opening between 0.04 to 0.4, the thickness of this vortex is about 0.28 times the depth of the approaching flow (Rajaratnam and Humphries, 1982).

2.4.3. Surface film

When water flows at low velocities in a laboratory flume up against a barrier that detains the surface, surface-active agents naturally present in the water rise to the surface and form a film on the upstream side of the barrier. The surface film is characterized by a faint line or ripple barely visible on the water surface at its leading edge (Harber and Gulliver, 1992). This line is known as Reynolds-ridge.

2.4.4. Upstream flow velocity

Velocity field is the most important property of flow. In fact, determining the velocity is, in many cases, solving a flow problem, since other properties follow directly from it (White, 2003). Velocity distribution upstream of vertical sluice gate was first investigated by Rajaratnam and Humphries (1982). They present experimental measures of velocity profile at a longitudinal distance from the gate of 10, 50 and 100 cm with 5 cm of gate opening and approximately 40-42 cm of water depth. Figure 2.5 shows Rajaratnam and Humphries (1982) experimental measures.

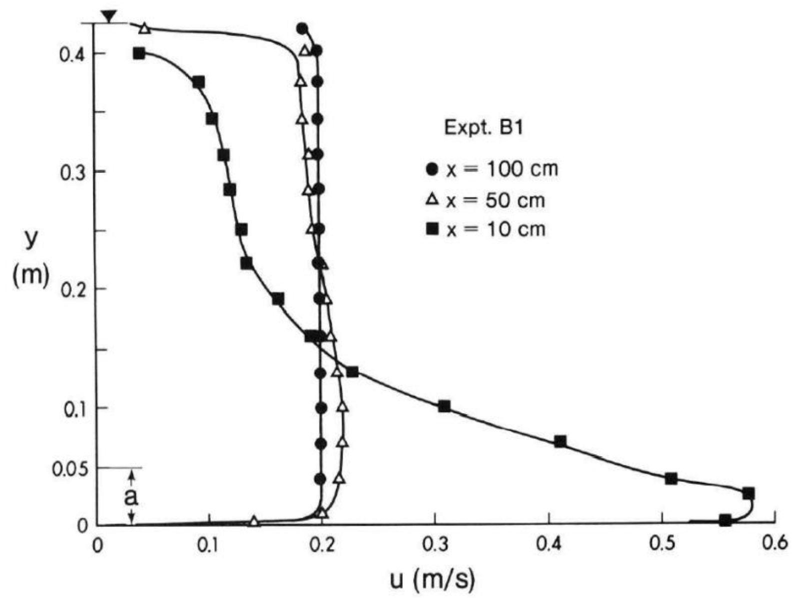

Figure 2.5 Typical velocity profile upstream of the gate
(Rajaratnam and Humphries, 1982).

For a ratio between longitudinal distance upstream of gate and gate opening less than about 4 (x/a<4), the velocity profile had the typical (plane) wall jet profile wherein longitudinal component of velocity increases with depth up to a maximum velocity at y=δ and then decreases as water depth increases further (Rajaratnam and Humphries, 1982). Later studies present the same shape of velocity profile in converging flow region (Masliyah *et al.* 1985, Finnie and Jepson 1991, Montes 1997, Roth and Hager 1999, Shamma *et al.* 2005, among others). However, no agreement has been reached on what the influence really is, how far it goes, what characteristics it involves, etc.

2.5. Tailgate

It is known that a control gate may be fitted to control the flow depth, or setting the tailwater level in the model or flume. A variety of so-called tailgates or other control structures can be used to control the tailwater level. The tailgate should be strong and easy to adjust under load, and it should be far enough downstream so that backwater effects do not affect the depth and velocity distribution at the measurement section (Muste *et al*. 2017).

A wide range of gates for this purpose are available, all of them have a main characteristic in common, flow blockage is partial, making streamlines converge: at the bottom (planar vertical or inclined sluice gate, radial or sector gates), at water free surface (crest gates or weirs, flap gates), beside (planar skew gates) at the flow centerplane (mitre gate), etc. The novelty of this work is uniform vertical blockage of flow allowed by double louver gate.

2.6. Double louver gate (DLG)

The double-louver gate consists in two plates, one fixed and one vertically adjustable for control of discharge and upstream flow depth. Both of these plates have multiple openings like a louver. The relative position of adjustable plate regarding to fixed one uncover those openings and allows the discharge Figure 2.6 shows a scheme of this gate.

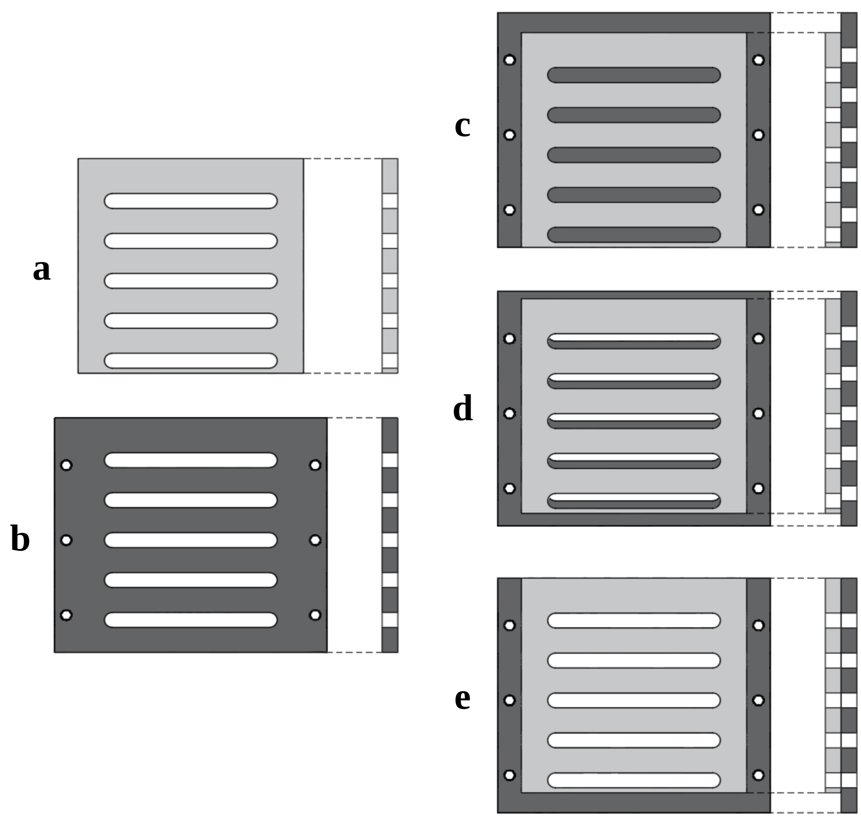

Figure 2.6 Front and side view of **a** Adjustable louver plate of DLG. **b** Fixed louver plate of DLG. **c** Fully closed configuration. **d** Partially open configuration. **e** Fully opened configuration.

2.7. Particle image velocimetry

PIV consists on incorporate small tracer particles to the flow, they were then illuminated using a plane of light and their motion was recorded with a camera. The recorded videos are processed to identify the motion and displacement of groups of particles by using cross correlation between two sequential frames. Once the displacements are calculated, and knowing the time elapsed between frames, the velocity field can be calculated. The information given by the velocity field is post-processed to describe flow and vortex characteristics. Figure 2.8 shows PIV scheme.

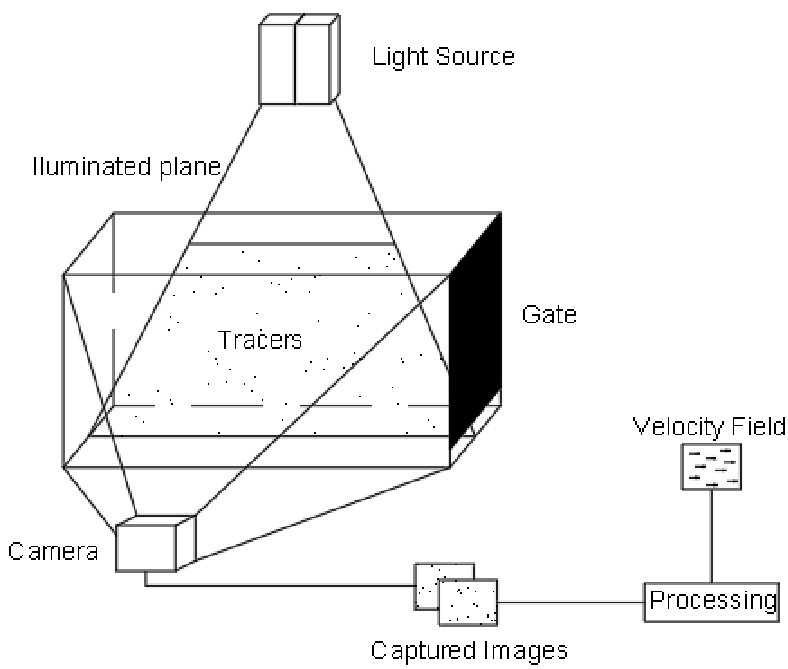

Figure 2.7 Particle Image Velocimetry measure technique scheme.

CHAPTER 3. MATERIAL AND METHODS

3.1. Introduction

This chapter describes the experimental setup developed to measure upstream characteristics of both studied gates. In order to accomplish this, the detailed description of studied gates, flume circuit, flow measurement method, post processing and experimental series configuration are presented.

3.2. Experimental installation

Experiments were carried out in a rectangular channel, 6 m long, 40 cm wide and 40 cm deep at the Laboratory for Hydraulic Engineering at Universidad de Concepción. To guarantee an aligned flow and eliminate large eddies in the incoming flow, a honeycomb matrix was placed at the flume entrance. After the endgate the flow falls into a tank where a 3-kW pump with 17 l/s capacity impulse it to a recirculation conduct.

A variable frequency drive was used to set different discharges in the hydraulic system through a change of the frequency rotation of the pump impeller. A step motor was used to adjust the opening of the endgate.

Both, the variable frequency drive and the step motor were controlled by a programmable logic controller (PLC).

A heat exchanger was used to keep the water temperature constant during the experiments, avoiding changes in the water viscosity. Experimental setup is shown schematically in Figure 3.1.

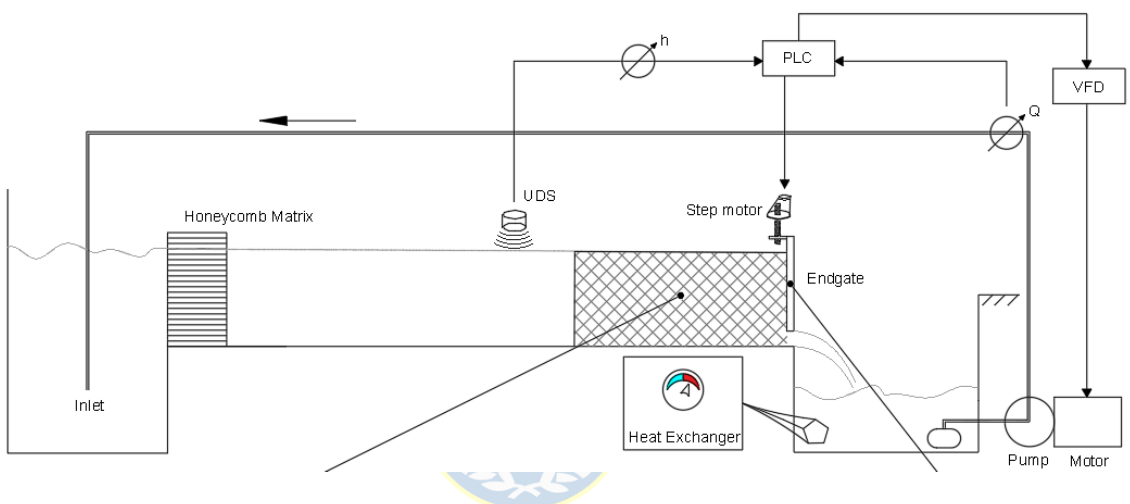

Figure 3.1 Schemes of the experimental installation.

Experiments were conducted with two different gates, namely a wooden broad edged sluice gate, 41 cm wide and 1 cm thickness, and a high-density PVC, double-louver gate wherein each louver has 11 openings of 1.5 cm separated by 2 cm between them, and those openings has 37 cm in width. Figure 3.2 exposes DLG geometric properties used.

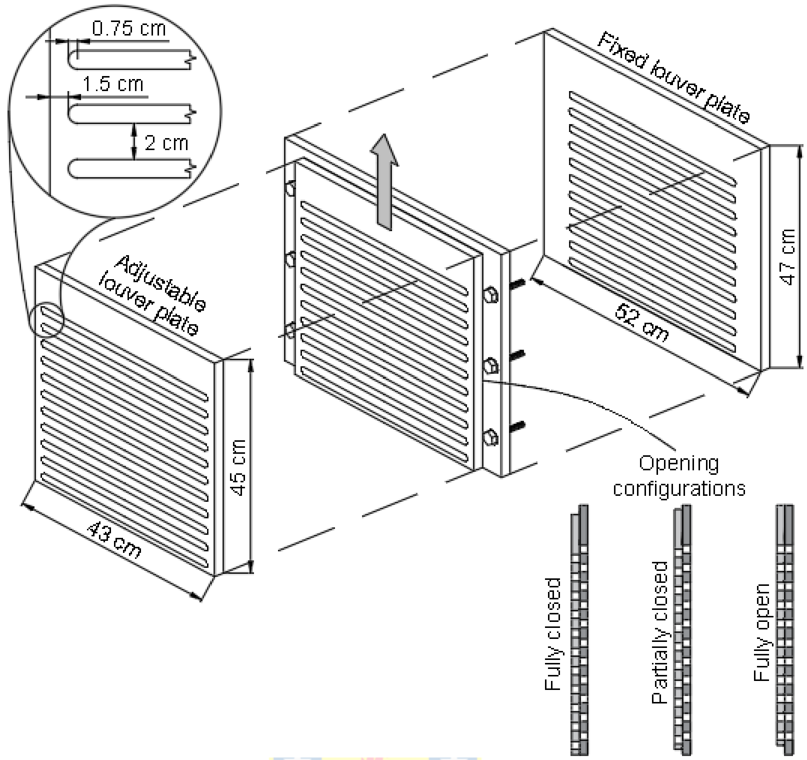

Figure 3.2 Double louver gate dimensions and design.

3.3. Measuring techniques

Discharge was measured with an electromagnetic flow meter having an accuracy of ±0.5%. The flow depth was measured with an ultrasonic distance sensor (UDS). The velocity field was measured using a Particle Image Velocimetry (PIV) system. A GoPro Hero 5 Black with a 32GB memory, 4000x3000 pixels max resolution (12 MP) and acquisition frequency of 120 Hz was used to record the digital images. Two sources of light were used as the light density of a single one was not enough to produce a good contrast level in the images. The light was collimated to illuminate 20 cm long 0.5 cm wide windows along the flume. Polyamide-12 particles of 100 μm diameter and 1.06 g/cm3 density were used. The particles material and white color allow a high-performance scattering of the light source. The displacements of the flow tracers were determined using the toolbox for Matlab, PIVlab® version 2.38 developed by Thielicke and Stamhuis (2014a).

Motion recorded and images obtained was converted into a grayscale through MATLAB in order to reduce its size and then was loaded in PIVlab toolbox with a time resolved image sequencing style. A total of 30 images (29 frames) was used in each analysis.

Region of interest was selected and no mask was used. Only a contrast limited adaptative histogram equalization (CLAHE) was applied to all frames in order to improve grayscale contrast. In this particular image pre-procesing technique, the contrast of every tile is optimized by histogram equalization, so that the resulting distribution matches a flat shaped histogram ranging from 0 to 255. Regions with low exposure and regions with high exposure are therefore optimized independently. After the histogram equalization, all neighbouring tiles are combined using a bilinear interpolation, resulting in an image without visible boundaries between the tiles (Thielicke, 2014). Windows size chosen was 20 pixels.

Small sub images (interrogation areas) of an image pair are cross-correlated to derive the most probable particle displacement in the interrogation areas. In essence, the cross-correlation is a statistical pattern matching technique that tries to find the particle pattern from interrogation area A back in interrogation area B (Thielicke, 2014). A Fast Fourier Transform windows deformation technique with a multi-pass approach was used. First pass used was large to capture high velocity flow information and then interrogation size was gradually decreased in the next passes.

The integer displacement of two interrogation areas can be determined straightforward from the location of the intensity peak of the correlation matrix. The peak of the fitted function is used to determine the particle displacement with subpixel precision (Thielicke, 2014). The subpixel estimator technique chosen was Gauss 2x3 point fit.

After the analysis finishes, next step was a calibration of the data. A 200 mm reference distance corresponding to water depth and 33.33 ms time step corresponding to time from one image to the other image was applied for calibration. Thereafter a vector validation was also applied to all frames to rid atypical vectors or other errors come from correlation.

For a visualization of recirculation zones or eddies at the upper part of the gates, a particle tracing technique was used, which consists in images with a long exposure to light.

3.4. Experimentation

After introducing a constant flow rate into the flume, the gates were open to set a flow depth of 20 cm. In all experiments water temperature was set at 20°C. Under such conditions, the sluice gate opening was 1.7 cm corresponding to 8.5% of the flow depth, while double-louver gate has 5 openings under water level with a partial opening of 6 mm each, which in total corresponds to 33% of the flow depth. Table 1 shows the conditions of the experiments.

Table 3.1. Experimental runs.

Run	Gate	a/h_0 (%)	Q (l/s)	h_0 (cm)	U_0 (m/s)	R	F	T (°C)
A	VSG	8.5	8.8	20	0.110	44000	0.0079	20
B	DLG	33	8.8	20	0.110	44000	0.0079	20

CHAPTER 4. RESULTS

4.1. Introduction

This chapter presents the flow properties, including identification of recirculation zones, vertical velocity profiles, and distribution of turbulent kinetic energy. The comparative advantages/disadvantages of the double-louver gate respect to the vertical sluice gate are briefly discussed.

4.2. Observations

Recirculation zone, location of vortex structure and particles paths are shown in Figure 4.1 for x = 0 to 6.7 times the vertical sluice gate opening. Clearly, in the VSG case the vertical component of the velocity is important, and a recirculation zone develops close to the gate below the water surface. Instead, in case of the DLG, streamlines remain parallel and horizontal, without important vertical deviations. A small recirculation zone close to the gate below the water surface was observed only when the gate blocked the upper flow layer.

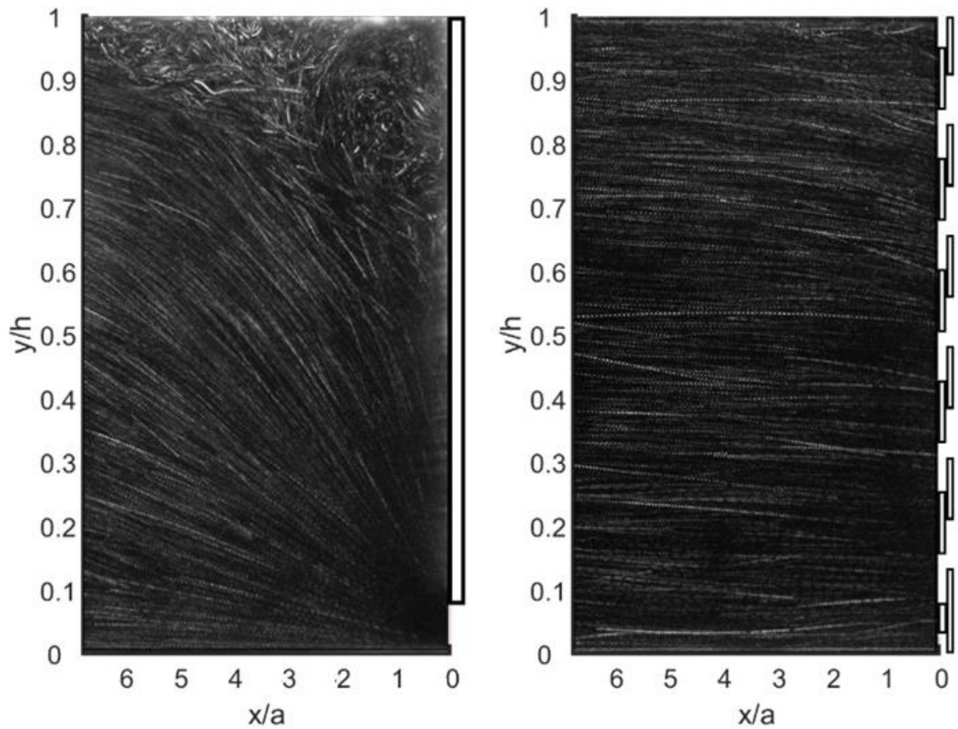

Figure 4.1 Particle tracing upstream of VSG and DLG.

4.3. Flow field

Figure 4.2 shows velocity field, velocity vector direction and TKE upstream of the VSG and DLG. For the VSG longitudinal velocities increase to the bottom, and negative values close to the gate, below the surface evidence the observed recirculation zone. For the DLG the maximum horizontal velocity is observed in the center of the water column, diminishing to the water surface and channel bottom, resembling the properties of a bounded velocity profile. Consistently to the formation of a recirculation zone close to the VSG below the surface, velocity vector direction shows values in the range between 0 and 360°. In case of the DLG, velocity vector directions are close to zero everywhere, confirming the absence of a vertical velocity component.

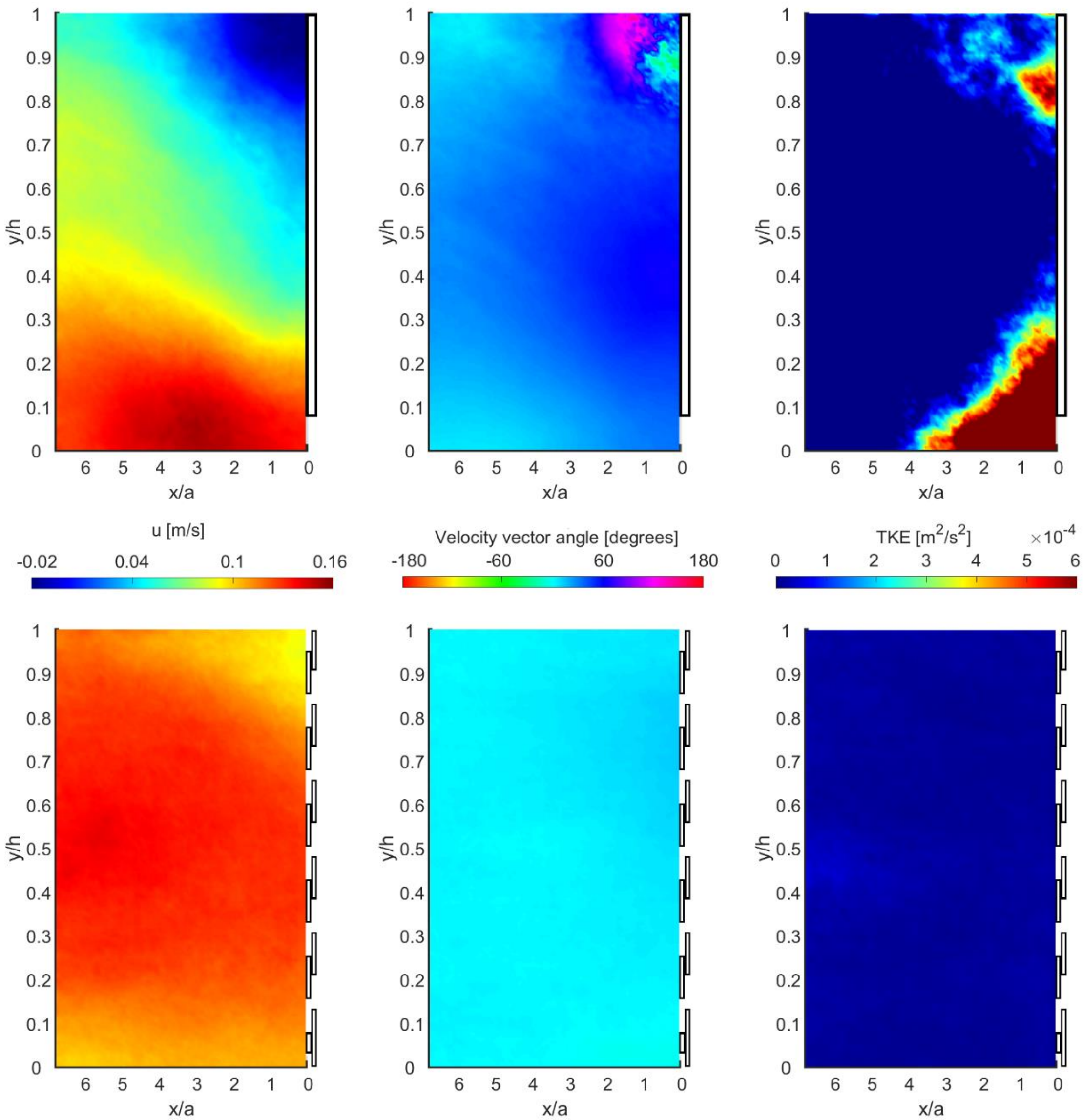

Figure 4.2 Velocity field (left), velocity vector direction (center) and TKE (right) upstream of VSG (upper panel) and DLG (bottom panel).

Two cores of turbulent kinetic energy are observed in the case of the VSG: one corresponding to the recirculation zone close to the gate, below the surface, and another one associated with the flow concentration at the gate opening. In case of the DLG, the TKE distribution is quite homogenous in the measured window.

4.4. Vertical velocity profiles

Figure 4.3 shows normalized velocity profiles of the longitudinal and vertical components at different distances upstream the VSG and DLG. Measured values are compared with those by Akoz et al. (2009). For the VSG, the measured longitudinal velocity profile in the region close to the gate is in fair agreement with that by Akoz et al. (2009), exhibiting the typical plane wall jet profile reported by Rajaratnam and Humphries (1982). The DLG instead, produces a velocity profile that resembles the logarithmic profile, showing negligible alteration to the open channel flow. Longitudinal velocities are lower than those by Akoz et al. (2009), which is attributed to the relative gate opening a/h_0, which in the present study was 0.085, while in

Akoz et al. (2009) was 0.112. Consistently, vertical velocity component close to the gate is very small in the DLG compared to the VSG.

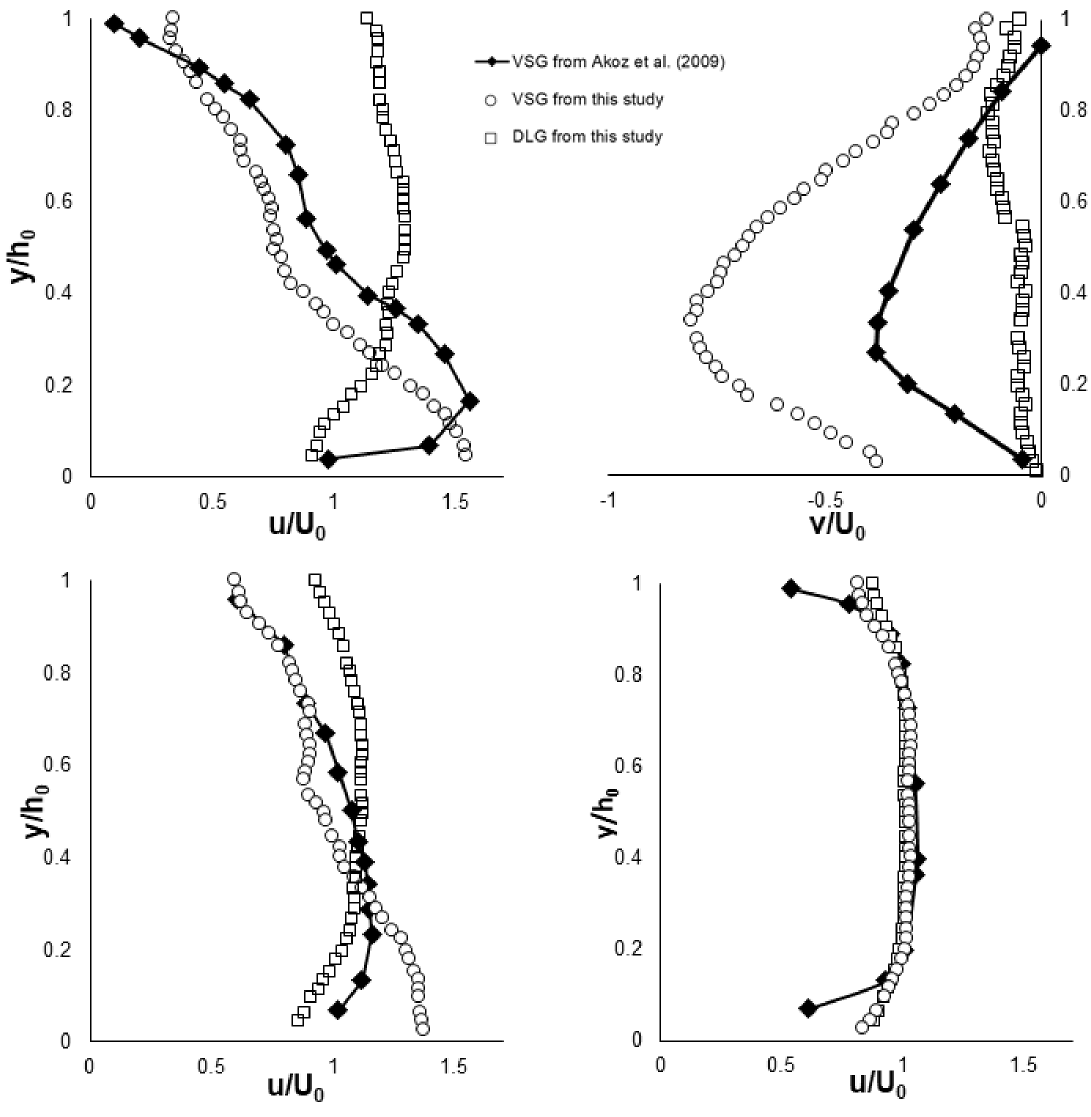

Figure 4.3 Normalized velocity profiles of the longitudinal and vertical components close to the gate at x=3.67a, and far from the gate at x=7a y x=10.33a for VSG and DLG. Measured values are compared with those by Akoz et al. (2009).

Figure 4.4 shows the normalized stream-wise velocity profiles upstream from DLG and VSG against the relative water depth y/h_0. A plane wall jet vertical distribution is observed upstream of the VSG, evidencing the influence of the gate on the flow field. The recirculation zone below the surface is observed upstream the gate up to a distance of x = 12a.

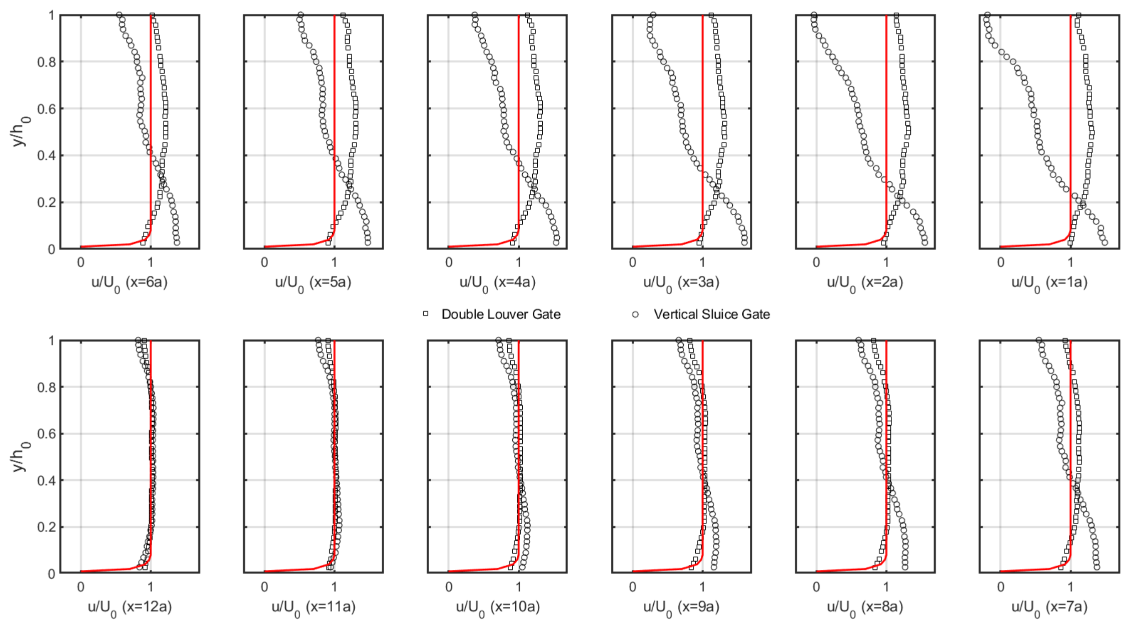

Figure 4.4. Velocity profiles for x=a to x=12a upstream of DLG and VSG.

Figure 4.5 shows the root mean square error of the measured velocity distributions with respect to the theoretical logarithmic profile for both gates. The velocity distribution upstream of the DLG was similar and much closer to the logarithmic profile than that upstream of the VSG. In both cases, RMSE increased towards the gates.

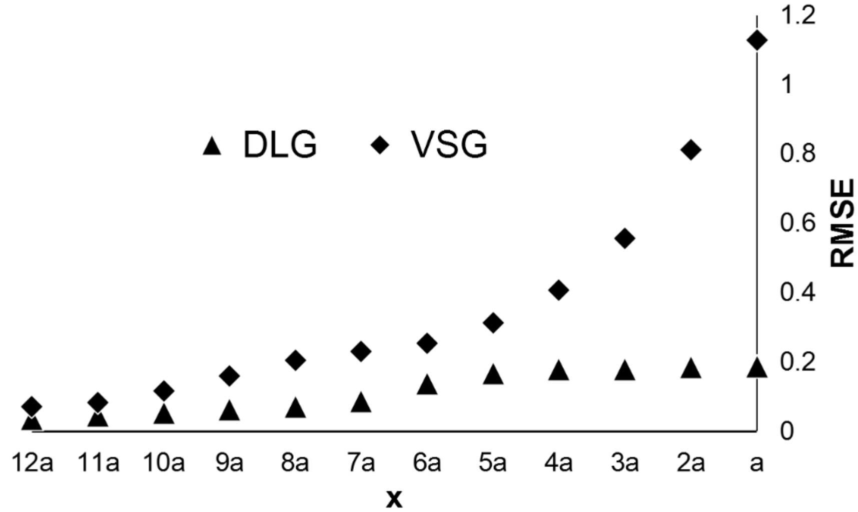

Figure 4.5 RMSE for x=a to x=12a upstream of DLG and VSG.

CHAPTER 5. CONCLUSION

The effects of a double louver gate on the upstream flow in a laboratory flume were analyzed through a particle image velocimetry. Vertical velocity profiles, recirculation zones, and turbulent kinetic energy distributions showed that the double louver gate is less flow-altering than the common vertical sluice gate, being best suited for the outflow control in flumes, as it conserves parallel streamlines, with a minimum deformation of the vertical velocity profiles, avoiding the formation of recirculation zones and concentrations of turbulent kinetic energy. Improvement in any part of experimental set up would provide a more solid foundation for experimental findings, better approximations of real situation leading to improved design and cost reduction. Double louver gate is an improvement that will reduce uncertainly associated to tailgate upstream effect. Therefore, the double louver gate is recommended for its implementation in laboratory flumes.

REFERENCES

Akoz, M. S., Kirkgoz, M. S., & Oner, A. A. (2009). Experimental and numerical modeling of a sluice gate flow. Journal of Hydraulic Research, 47(2), 167–176.

Belaud, G., Cassan, L., & Baume, J.-P. (2009). Calculation of Contraction Coefficient under Sluice Gates and Application to Discharge Measurement. Journal of Hydraulic Engineering, 135(12), 1086–1091.

Boiten, W. (2002). Flow measurement structures. Flow Measurement and Instrumentation, 13(5-6), 203–207.

Cassan, L., & Belaud, G. (2012). Experimental and Numerical Investigation of Flow under Sluice Gates. Journal of Hydraulic Engineering, 138(4), 367–373.

Dazzi, S., Vacondio, R., & Mignosa, P. (2020). Internal boundary conditions for a GPU-accelerated 2D shallow water model: implementation and applications. Advances in Water Resources. 103525.

Finnie, J. I., & Jeppson, R. W. (1991). Solving Turbulent Flows Using Finite Elements. Journal of Hydraulic Engineering, 117(11), 1513–1530.

Harber, C. D., & Gulliver, J. S. (1992). Surface films in laboratory flumes. Journal of Hydraulic Research, 30(6), 801–815.

Henderson F. M. (1966). Open channel flow. Macmillan Publishing Co, Inc. New York.

Masliyah, J. H., Nandakumar, K., Hemphill, F., & Fung, L. (1985). Body-

Fitted Coordinates for Flow Under Sluice Gates. Journal of Hydraulic Engineering, 111(6), 922–933.

Montes, J. S. (1997). Irrotational Flow and Real Fluid Effects Under Planar Sluice Gates. Journal of Hydraulic Engineering, 123(3), 219–232.

Muste M., Lyn D. A., Admiraal D. M., Ettema R., Nikora V. & García M. H. (2017). Experimental Hydraulics: Methods, Instrumentation, Data Processing and Management. Volume I: Fundamentals and Methods. CRC Press. London. UK.

Rady, R. A. E.-H. (2016). Modeling of flow characteristics beneath vertical and inclined sluice gates using artificial neural networks. Ain Shams Engineering Journal, 7(2), 917–924.

Rajaratnam, N. (1977). Free flow immediately below sluice gates. Journal of Hydraulics Division, 103(HY4), 345–351.

Rajaratnam, N., & Humphries, J. A. (1982). Free Flow Upstream of Vertical Sluice Gates. Journal of Hydraulic Research, 20(5), 427–437.

Rajaratnam, N., & Subramanya, K. (1967a). Flow equation for the sluice gate. Journal of Irrigation and Drainage Division. 93(3), 167–186.

Rajaratnam, N., and Subramanya, K. (1967b). Flow immediately below a submerged sluice gate. Journal of Hydraulics Division. 93(HY4), 57–77.

Roth, A. and Hager, W. H. (1999). Underflow of standard sluice gate. Experiments in Fluids, 27, 339 350.

Shammaa, Y., Zhu, D. Z., & Rajaratnam, N. (2005). Flow Upstream of Orifices and Sluice Gates. Journal of Hydraulic Engineering, 131(2), 127–133.

Thielicke, W. (2014): The Flapping Flight of Birds - Analysis and Application. Phd thesis, Rijksuniversiteit Groningen.

Thielicke, W., Sonntag, R. (2021) Particle Image Velocimetry for MATLAB: Accuracy and enhanced algorithms in PIVlab. Journal of Open Research Software, 9: 12.

Thielicke, W. and E. Stamhuis (2014). PIVlab – Towards User-friendly, Affordable and Accurate Digital Particle Image Velocimetry in MATLAB. Journal of Open Research Software. 2(1). e30 1-10.

White F. M. (2003). Fluid Mechanics. McGraw-Hill. New York.

Wu, S., & Rajaratnam, N. (2015). Solutions to Rectangular Sluice Gate Flow Problems. Journal of Irrigation and Drainage Engineering, 141(12), 06015003.